REGULAR PAPER

A Study on the Effects of Specimen Geometry on Measurement Accuracy of Dynamic Constitutive Properties of Metals Using SHTB

Khac-Ha Nguyen[1] · Chang-Whan Lee[2] · Hyunho Shin[3] · Joo Hyoung Lee[4] · Jong-Bong Kim[5]

Abstract

Determination of dynamic tensile response of materials has been a challenge because of experimental difficulty. The split Hopkinson tensile bar (SHTB) is one of the most widely used devices for characterization of various materials under dynamic-tensile loading conditions. Since one-dimensional wave propagation in bars is disturbed by specimens and grips, however, SHTB measurement accuracy may not be guaranteed. This means that the stress–strain curve of the specimen that is calculated using strains at bars may not indicate the real stress–strain relation of the specimen. In this study, simulations for the SHTB test were carried out to investigate the effects of thread pitch, specimen length, specimen diameter, and thread inner diameter of the specimen on the measurement accuracy for two types of metals with medium and high yield strengths. Finally, specimen shapes are recommended for accurate measurement of the stress–strain relation of tantalum and tungsten carbide.

Keywords Split hopkinson tensile bar · High strain rate · Tantalum · Tungsten carbide

1 Introduction

The split Hopkinson bar (SHB), first introduced by Kolsky [1], is the most commonly applied technique to study material behaviors under high rate deformation. The SHB was originally designed for measurement of dynamic constitutive properties in compression condition. The need for

✉ Hyunho Shin
hshin@gwnu.ac.kr

✉ Jong-Bong Kim
jbkim@seoultech.ac.kr

1 Department of Automotive Engineering, Seoul National University of Science and Technology, Seoul 01811, Korea

2 Department of Mechanical System Design Eng, Seoul National University of Science and Technology, Seoul 01811, Korea

3 Department of Materials Engineering, Gangneung-Wonju National University, Gangneung-si 25457, Gangwon-do, Korea

4 Agency for Defense Development, Daejeon 34186, Korea

5 Department of Mechanical and Automotive Engineering, Research Center for Electrical and Information Technology, Seoul National University of Science and Technology, Seoul 01811, Korea

in-depth study of the high-strain-rate deformation mechanisms of materials motivated the development of various types of SHB apparatus. In general, SHB techniques are classified into torsion (SHToB) [2, 3], tension (SHTB), and compression (SHPB) split Hopkinson bars [4–13]. In the SHB technique, a short cylindrical specimen is sandwiched between incident and transmit bars. When a striker is fired at an incident bar, a stress wave propagates upon impact along the incident bar. At the end of the incident bar, a part of the stress is reflected because of impedance mismatch between the bars and the specimen. A part of the stress wave keeps transmitting to the transmit bar until it reaches the end of the bar. The strain and stress of the specimen are calculated using strains measured at the incident and transmit bars, respectively. Lei and Xu [7] modified the Johnson–Cook (JC) [8] constitutive model and determined the model coefficients of cupronickel B10. Shin and Kim [9] studied the long duration time of the transmit pulse when a soft specimen was tested. Chunzheng et al. [10] carried out SHPB testing to derive the dynamic recrystallization temperature. Kim et al. [11] used self-organizing map analysis and SHPB to study the damage mechanisms in armor structural materials under high strain rate deformation.

Recently, measurements of dynamic constitutive properties in tensile condition have been studied. Several specimen

and grip shapes were proposed for SHTB. Lindholm and Yeakley [12] carried out SHTB with hat type specimens and compared their results with those of SHPB. Staab and Gilat [13] investigated the effect of bar type specimens in SHTB tests. When the length to diameter ratio of a specimen is larger than or equal to 1.6, the experimental results show that the dynamic tensile strength is consistent for repetitive experiments. Bang and Cho [14] studied the failure behavior of fabric reinforced polymer matrix composite via SHTB. Huh et al. [15] used bolts to fix sheet type specimens. Using SHTB, Nicholas [16] employed threaded specimens to determine stress–strain curves for more than 20 different materials.

Most of these studies were carried out only by experiment; validation of SHTB was not performed. In contrast to the compressive test, a special method to fix specimens to bars, such as grips or bolts, is needed, so that tensile stress waves can transfer through the grip between bars and specimens in SHTB. Using a bolted grip assembly, Pham et al. [17] numerically studied measurement errors in SHTB. Nguyen et al. [18] investigated the effect of thread geometry on the stress wave propagation characteristics from the incident bar to the transmitter bar. In this research, proper thread geometries were proposed to transfer the incident stress wave to the transmit bar with minimum distortion in the SHTB apparatus. Prabowo et al. [19] simulated several sets of SHTB cases with dumb-bell shaped specimens, and showed that the stress–strain relation can be measured when the length-to-diameter ratio of the specimen is 0.75. This paper studied only the length-to-diameter ratio of the specimen; other crucial specimen geometries such as grip structure were not clarified.

In this study, with the development of numerical analysis such as the finite element method, the measurement accuracy of the dynamic constitutive properties measured using SHTB is investigated numerically based on the work of Nguyen [20]. Also, the effects of specimen geometries, such as specimen length, specimen diameter, thread pitch, and thread inner diameter on measurement accuracy are investigated. Finally, specimen geometries to secure the measurement accuracy in SHBT testing are proposed.

2 Principle of Split Hopkinson Tensile Bar

2.1 Split Hopkinson Tensile Bar System

A schematic illustration of the SHTB employed in this study is shown in Fig. 1. The main parts of the apparatus are an incident bar, a transmit bar, a striker tube, and a specimen. The striker tube is fired so as to impact the incident bar. From the impact, a tensile pulse is generated in the incident bar and propagates to the specimen. When the pulse reaches
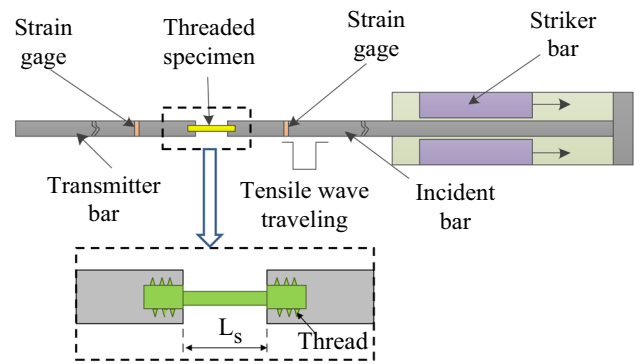

Fig. 1 Schematic illustration of SHTB system

the specimen, which is sandwiched between the incident and transmit bars, a part of the incident pulse is transmitted to the specimen and propagates to the transmit bar as a tensile pulse. The rest of the pulse reflects to the incident bar as the compressive pulse. The transmitted and reflected pulses are measured by strain gages attached to the two bars. The stress and strain of the specimen are calculated using the strains measured at the transmit (transmitted wave) and incident (reflected wave) bars, as follows:
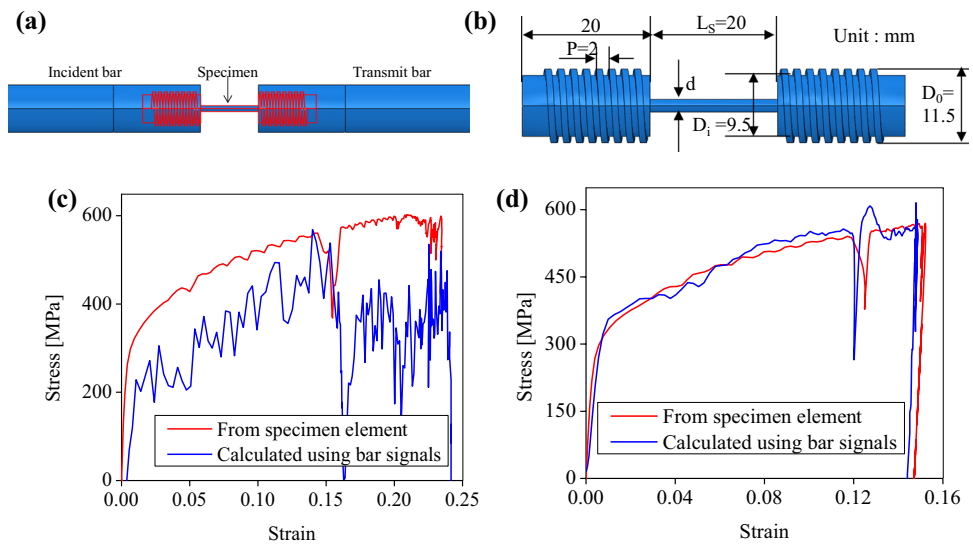
$$\sigma(t) = \frac{A_0}{A} E_0 \varepsilon_T(t) \tag{1}$$

$$\varepsilon(t) = -2\frac{C}{L_s} \int_0^t \varepsilon_R(\tau)d\tau. \tag{2}$$

In Eqs. (1) and (2), E_0 is the elastic modulus of the bars. A_0 and A are the cross-sectional areas of the bar and the specimen, respectively. ε_T and ε_R are the transmitted and reflected strains measured at the transmit and incident bars, respectively. C is the wave speed and L_S is the specimen length. Equations (1) and (2) were derived with assumptions of one-dimensional wave propagation and complete contact condition of specimen with the two bars.

Nguyen et al. [18] studied the measurement error when the specimen is not properly designed, as shown in Fig. 2. They carried out simulations for SHTB test using ABAQUS/Explicit. Figure 2a provides a detailed view of the assembled specimen and bars, utilizing a screw fixing. Specimen dimensions are shown in Fig. 2b. In the simulation, stress and strain can be obtained by monitoring the specimen elements or by calculation using Eqs. (1) and (2). Figure 2c, d show a comparison of the stress–strain relations calculated using Eqs. (1) and (2) and obtained (monitored) directly from the specimen for specimen diameters of 2.0 and 8.0 mm, respectively. It can be seen that it is possible to measure the stress–strain relation accurately when the specimen diameter is 8.0 mm, while

Fig. 2 Examples of measurement error: **a** schematic illustration of screw fixing, **b** dimensions of specimen, and **c**, **d** comparison of calculated (using incident and transmitter bar strains) stress–strain relation with that monitored from specimen for specimen diameters of 2.0 and 8.0 mm, respectively

Fig. 3 Definitions of strain error ($\Delta\varepsilon$) and area discrepancy ratio (η)

a large discrepancy between the measured and monitored curves is found when the specimen diameter is 2.0 mm. In contrast to SHPB, therefore, proper design of the specimen shape is needed in SHTB. In this study, therefore, simulations were carried out for SHTB using ABAQUS/Explicit; proper design of specimen shapes was also carried out.
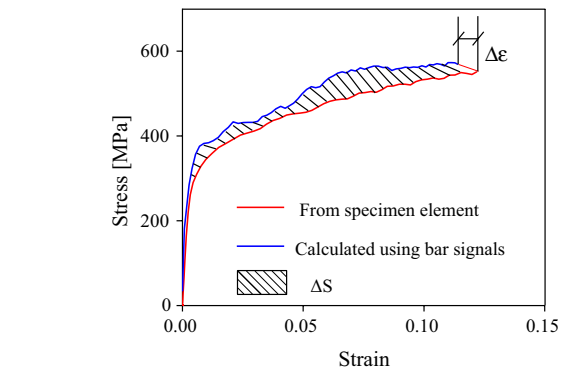
For all of the simulation in this study, the diameter and length of incident and transmitter bars are 16.0 and 2000.0 mm, respectively; the inner diameter, the outer diameter, and the length of striker bar are 16.1, 30.0, and 300.0 mm, respectively; the strain gages are attached in the middle of the incident and the transmitter bars.

2.2 Error Definition and Material Model

Since grip structures such as threads may distort one-dimensional wave propagation between bars and specimen, a specimen stress–strain curve calculated from strain at bars (ε_{cal}) may not match a curve directly monitored at the specimen (ε_{mo}). To evaluate the SHTB measurement accuracy, two types of error are defined, as shown in Fig. 3. The first is the total axial strain difference between calculated strain (ε_{cal}) [obtained using Eq. (2)] and monitored strain (ε_{mo}) at the specimen, as follows:

$$\Delta\varepsilon = \left| \varepsilon_{cal} - \varepsilon_{mo} \right| \tag{3}$$

In Eq. (3) ε_{cal} and ε_{mo} are the total strains (calculated and monitored, respectively) of the specimen up to necking. The second one is the 'area discrepancy ratio (η)', which was defined as the ratio of area discrepancy of the stress–strain curve to the true area of the stress–strain curve, as follows:

$$\eta = \frac{\int_0^\varepsilon \left| \sigma_{cal} - \sigma_{mo} \right| d\varepsilon}{\int_0^\varepsilon \sigma_{mo} d\varepsilon} \tag{4}$$

In Eq. (4) σ_{cal} is the calculated stress using Eq. (1), and σ_{mo} is the stress monitored at the specimen. The strain error $\Delta\varepsilon$ and the area discrepancy ratio η are used to evaluate the measurement accuracy of the test. In this study, specimen characteristics such as thread shapes, specimen diameter, and specimen length are chosen to minimize the measurement error.

The Johnson–Cook (JC) constitutive model is used to describe the plastic behavior of bars and specimen. This model is described by Eq. (5).

$$\sigma = (A + B\varepsilon^n)\left(1 + C \ln \left(\frac{\dot{\varepsilon}}{\dot{\varepsilon}_0} \right) \right)(1 - T^{*m}), \tag{5}$$

where T^* is the homologous temperature given by Eq. (6).

$$T^* = \frac{T - T_o}{T_{melt} - T_o}. \tag{6}$$

where T is the temperature of the specimen, T_0 is the reference temperature, and T_{melt} is the melting temperature of the specimen. The JC model contains five material constants, A, B, n, C, and m. Simulations for SHTB were carried out for two types of material, i.e., tungsten carbide for relatively high strength and tantalum for relatively low strength. The JC model coefficients of AISI 4340 steel, tungsten carbide, and tantalum are shown in Table 1. The model coefficient of tantalum was determined [23, 24] using the data of Maudlin et al. [25] and Nemat-Sasser and Isaacs [26].

3 Effect of Specimen Geometries on Measurement Accuracy

The thread type specimen is shown in Fig. 4. The main parameters for specimen shape are thread inner diameter (D_i), pitch, specimen length, and diameter (D). According to the thread standard, the thread outer diameter is determined from the thread inner diameter and pitch. In this study, the effect of the abovementioned specimen geometries on measurement accuracy in SHTB is investigated. The effect of element size on the analysis results was first studied and proper size was used.

3.1 Thread Pitch

In the SHTB system, the thread pitch of the specimen affects the stress wave transmission through the specimen from the incident to the transmitter bars. To investigate the effects of thread pitch on measurement accuracy, simulations were carried out for specimens having thread pitches of 2.0, 2.4,
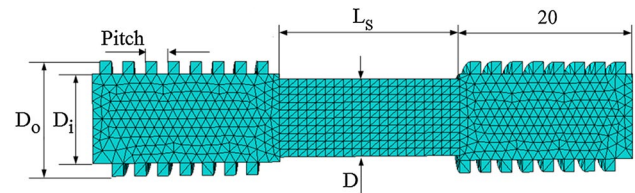

Fig. 4 Specimen shape and element discretization

2.8, and 3.2 mm. The thread inner diameter, specimen diameter, and striker velocity were 9.0 mm, 8 mm, and 20 m/s, respectively. The thread length was fixed at 20 mm. Figure 5 compares values of a stress–strain curve calculated using bar strains with values obtained directly from the specimen for thread pitches of 2.4 and 3.2 mm for tantalum. The strain rate is about 1100 s^{-1} for all of the analysis. It can be seen that the thread pitch affects the measurement accuracy. For a clearer understanding, the strain error and area discrepancy ratio are presented in Fig. 6. Nguyen et al. [18] mentioned that the plastic strain on the thread region has an effect on stress wave propagation through the thread. So, the maximum plastic strain in the thread region is also presented in Fig. 6. In Fig. 6, the strain error and area discrepancy ratio are lowest when thread pitch is 2.4 mm. Also, it is shown that the strain error and the area discrepancy ratio are highly dependent on the plastic strain of the thread region. As the maximum plastic strain of the thread region decreases, the measurement error decreases. Numerical analysis for SHTB were also carried out for tungsten carbide, which has relatively high yield strength. Figure 7 shows the strain error and area discrepancy ratio for tungsten carbide. For the tungsten carbide specimen, the thread inner diameter, the specimen diameter, the specimen length, and the striker velocity are 7.5 mm, 7 mm, 25 mm, and 20 m/s, respectively. Based on

Table 1 Material properties of bar and specimens

Property	Material		
	AISI 4340 [21]	Tungsten Carbide [22]	Tantalum [23–26]
Density [kg/m³]	7865	17,600	1897
Young's modulus [MPa]	200	389	100
Poisson's ratio	0.285	0.213	0.3
JC model coefficients			
A [MPa]	792	1050	185
B [MPa]	510	177	675
C	0.014	0.014	0.047
n	0.26	0.12	0.3
m	1.03	1	0.425
T_m [K]	1700	1723	3250
T_{Ref} [K]	298	298	298
$\dot{\varepsilon}_0$ [1/s]	1	1	1

Fig. 5 Comparison of monitored stress–strain curve with that calculated using bar strains for thread inner diameter of **a** 2.4 and **b** 3.2 mm (tantalum)
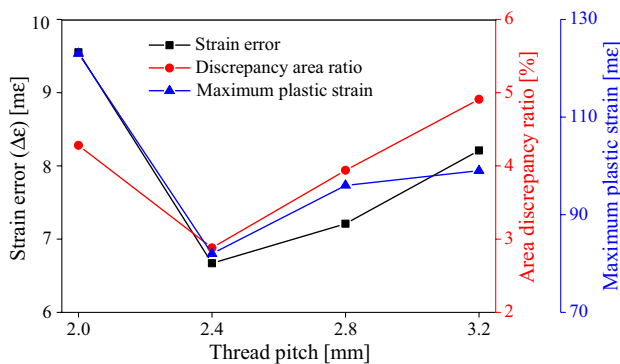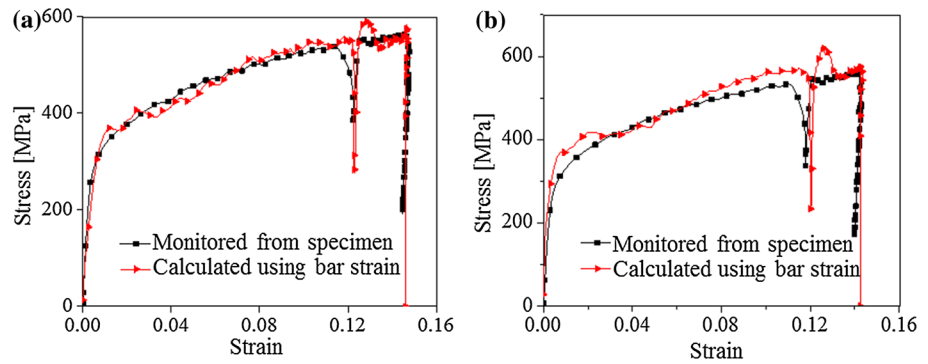
Fig. 6 Effect of thread pitch on measurement error and maximum plastic strain on thread region (tantalum)
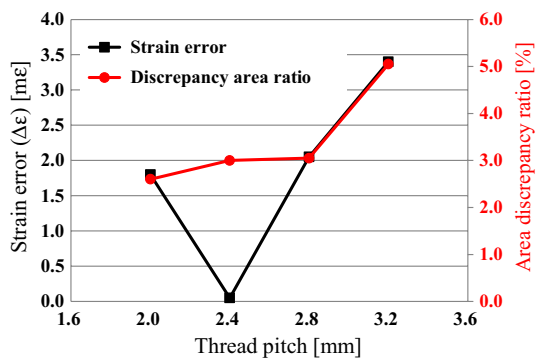
Fig. 7 Effect of thread pitch on measurement error on the thread region (tungsten carbide)

these results, the thread pitch of 2.4 mm was chosen for tantalum, and also for tungsten carbide in the next analysis.

3.2 Specimen Length

To investigate the effect of specimen length on the measurement accuracy, analyses were carried out for various specimen lengths in a range of 5 to 30 mm. For tantalum, thread pitch, thread inner diameter, specimen diameter, and striker velocity are 2.4 mm, 9.0 mm, 8.0 mm, and 20 m/s,

respectively. Figure 8 compares the stress–strain curve calculated using the bar strains with that monitored directly at the specimen for the specimen lengths of 5.0 and 25.0 mm. The strain rates are about 4300 and 1100 s^{-1} for the case of specimen length of 5.0 and 25.0 mm, respectively. As can be seen, the specimen length has a great effect on SHTB measurement accuracy. When the specimen length is 5 mm, the calculated total strain is far greater than the real (monitored) strain. The strain error and area discrepancy ratio for tantalum and tungsten carbide are presented in Fig. 9. For the case of tantalum, the strain error and area discrepancy ratio are low when the specimen length is 15 or 20 mm. For the case of tungsten carbide, the strain error is lower than 3 mm when the specimen length is greater than or equal to 10 mm. The area discrepancy ratio is between 2.0 and 3.2% for all cases. Based on these results, the specimen lengths were chosen as 20 and 25 mm for tantalum and tungsten carbide, respectively.

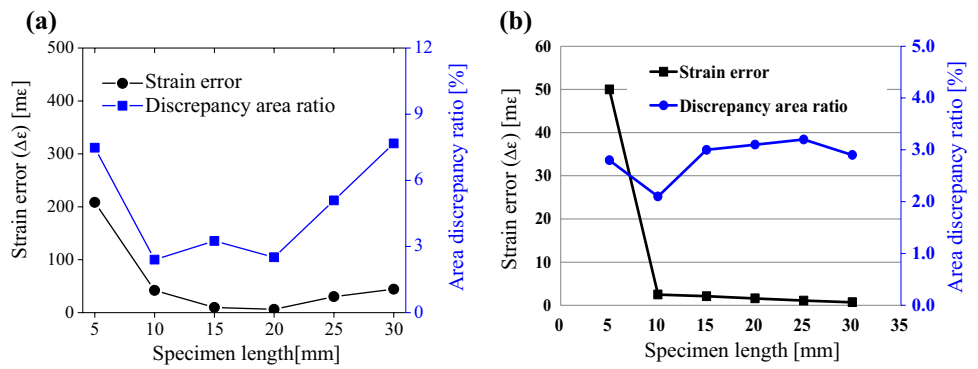### 3.3 Specimen Diameter and Thread Inner Diameter

Numerical analysis for SHTB were carried out for various specimen diameters from 4.0 to 9.0 mm. For tantalum, thread pitch, thread inner diameter, specimen length, and striker velocity are 2.4, 9, 20 mm, and 20 m/s, respectively. For tungsten carbide, thread pitch, thread inner diameter, specimen length, and striker velocity are 2.4, 7.5, 25 mm, and 20 m/s, respectively. For all of the analysis cases, the strain rate is about 1100 s^{-1}. The strain error and area discrepancy ratio of specimens are shown in Fig. 10. For tantalum, when the specimen diameter is 8 mm, the strain error and area discrepancy ratio are low. Therefore, the specimen diameter of 8.0 mm is recommended for tantalum. For the case of tungsten carbide, strain error is minimum when the specimen diameter is 7.0 mm. When the specimen diameter is 4.0 mm or 9.0 mm, both the strain error and the area discrepancy ratio become high.

Figure 11 shows the effect of thread inner diameter on the measurement accuracy. When the thread inner diameter is greater than or equal to 7.5 mm and lower than or equal to
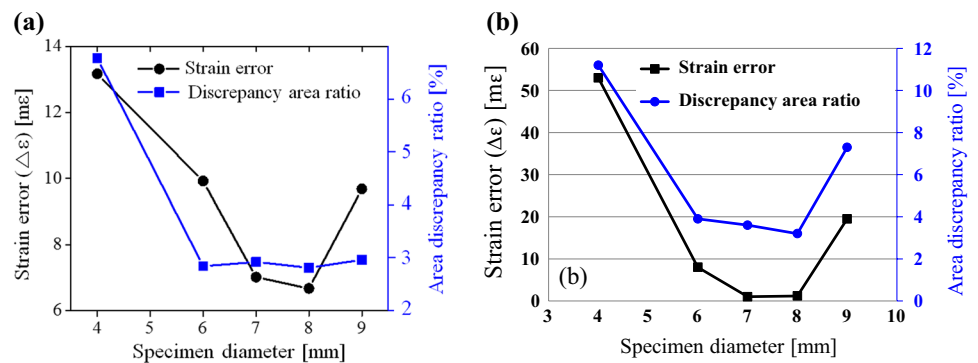
Fig. 8 Comparison of monitored stress–strain curve with that calculated using bar strains for specimen lengths of **a** 5.0 and **b** 25.0 mm (tantalum)
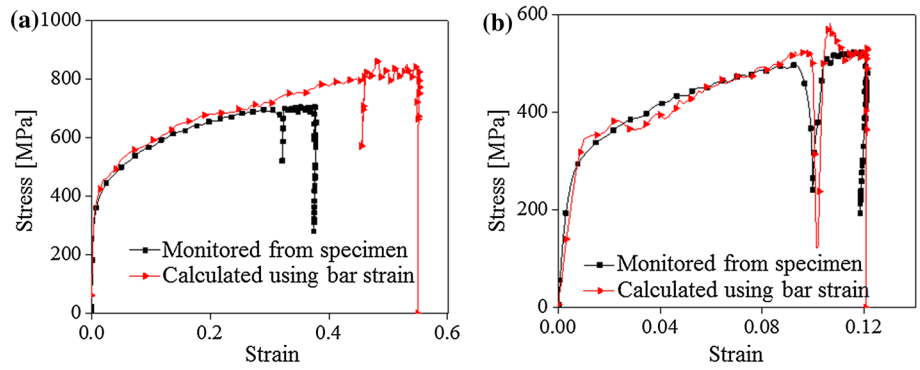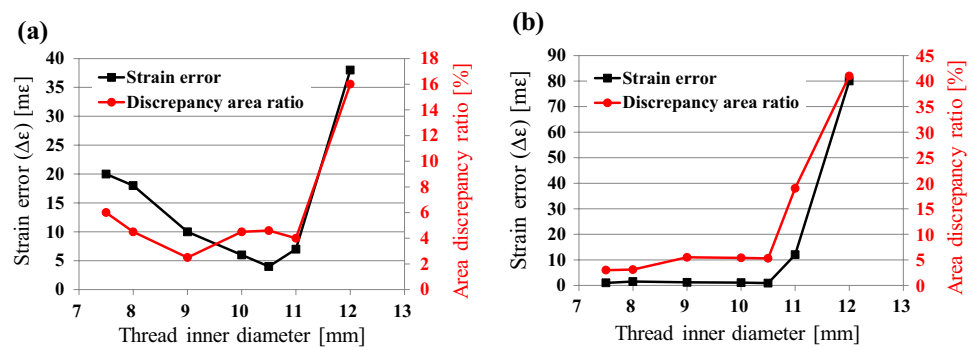

Fig. 9 Effect of specimen length on measurement error for **a** tantalum and **b** tungsten carbide

Fig. 10 Effect of specimen diameter on measurement error for **a** tantalum and **b** tungsten carbide

Fig. 11 Effect of thread inner diameter on measurement error for **a** tantalum and **b** tungsten carbide

to 10.5 mm, measurement errors are low compared to other cases. When the thread inner diameter is 12.0 mm, the thread region of the bars is too thin and large error is caused. Based on these results, 9.0 mm of thread inner diameter is recommended for both tantalum and tungsten carbide.

3.4 Discussions and Validation

In this study, the effects of specimen geometries such as thread pitch, thread inner diameter, specimen length, and specimen diameter on measurement accuracy were investigated. The strain error and area discrepancy ratio were found to have almost the same tendency. By looking at the values of the strain error for tantalum shown in Figs. 6, 9, 10, 11, it is shown that the specimen length and thread inner diameter have greater effects on the strain error and area discrepancy ratio than do the thread pitch and specimen diameter. For the case of tungsten carbide, shown in Figs. 7, 9, 10, 11, the effects of specimen diameter and thread inner diameter on strain error and area discrepancy ratio are greater than those of the thread pitch and specimen length.

Figure 12a shows the deformed shape and von-Mises stress distribution for the case in which the specimen length is 5.0 mm, as shown in Fig. 9a. It can be seen that too short a specimen length can fail to guarantee uniform deformation in the specimen region. So, 10–20 mm of specimen length is recommended. Figure 12b shows the deformed shape and von-Mises stress distribution for the case of that the specimen diameter is 4.0 mm in Fig. 10a. Local deformation takes place in some parts of the specimen and the uniform deformation assumption in the specimen region is not satisfied. To secure uniform deformation, therefore, a specimen diameter of greater than or equal to 6 mm is recommended. When the specimen diameter is greater than or equal to 9.0 mm, sufficient force to induce plastic deformation on specimen region cannot be transferred through the thread. This means that the force required to induce plastic deformation on the specimen also causes plastic deformation on the thread region; this is the main source of measurement error. So, a specimen diameter less than or equal to 8.0 mm is recommended.

Based on the simulation results, the recommended specimen dimensions are listed in Table 2. There are two main

Table 2 Recommended specimen geometries for tantalum and tungsten carbide. (unit: mm)

Parameter	Specimen material	
	Tantalum	Tungsten carbide
Thread pitch	2.4	2.4
Thread inner diameter	9.0	7.5
Specimen length	20.0	25.0
Specimen diameter	8.0	7.0

issues in the design of specimen dimensions. The first is to secure uniform deformation through the specimen. The second is that sufficient force should be transferred between the specimen and the bars, without plastic deformation on the thread region. Therefore, the recommended dimensions are not identical for the two materials. Considering the above mentioned issues, this means that the specimen shapes should be determined for each specimen materials.

To validate the measurement accuracy of the proposed specimen dimensions, simulations were carried out. Figure 13 shows the stress–strain relation for tantalum and tungsten carbide obtained using the dimensions in Table. 2. The strain errors are 4.2 and 1.5 mm for tantalum and tungsten carbide, respectively. The area discrepancy ratios are 2.8 and 2.6% for tantalum and tungsten carbide, respectively. As can be seen in Fig. 13, the measured stress–strain curves show values almost identical to those with that of monitored in the specimen.

4 Conclusions

The effects of specimen shape on measurement accuracy in SHTB were investigated. According to the analysis results, the following conclusions were drawn:

1. The strain error and area discrepancy ratio were defined to evaluate measurement accuracy in SHTB. The effects of pitch and inner diameter of thread, and length and diameter of specimen on the strain error and area

Fig. 12 Deformed shape and von-Mises stress distribution for cases of **a** specimen length of 5.0 mm, shown in Fig. 9a, b specimen diameter of 4.0 mm, shown in Fig. 10a
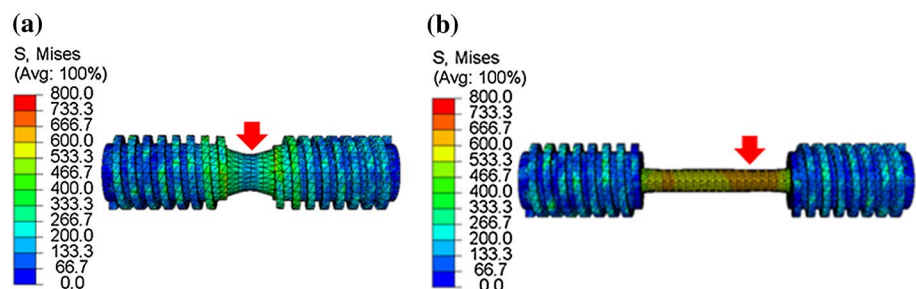
Fig. 13 Comparison of monitored stress–strain curve with that calculated using bar strains for **a** tantalum and **b** tungsten carbide with recommended specimen dimensions
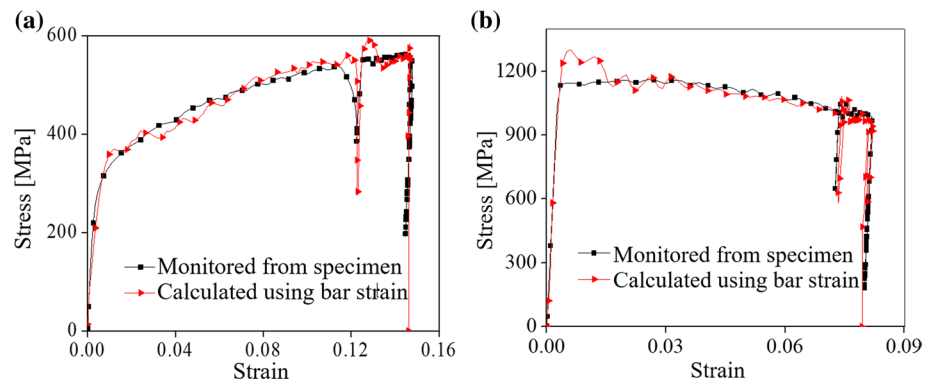
discrepancy ratio were investigated. Finally, dimensions of specimens with two different materials having medium (tantalum) and high (tungsten carbide) yield strength were recommended for SHTB to obtain high measurement accuracy.

2. For the case of tantalum, it is shown that the specimen length and thread inner diameter have greater effects on the measurement error than do the thread pitch and specimen diameter. For the case of tungsten carbide, the effect of specimen diameter and thread inner diameter on measurement error is greater than do the thread pitch and specimen length.

3. Dimensions of specimens were recommended for tantalum and tungsten carbide. Validation analyses for recommended dimensions were carried out. It is shown that, with the recommended specimen shapes, the dynamic stress-strain relation can be accurately measured in SHTB.

References

1. Kolsky, H. (1949). An investigation of the mechanical properties of materials at very high rates of loading. *Proceedings of the Physical Society B, 62*(11), 676–700.
2. Duffy, J., Campbell, J. D., & Hawley, R. H. (1971). On the use of a torsional split Hopkinson bar to study rate effects in 1100–0 Aluminum. *Journal of Applied Mechanics, 38*(1), 83–91.
3. Gilat, A., & Cheng, C. S. (2000). Torsional split Hopkinson bar tests at strain rates above $10^4 s^{-1}$. *Experimental Mechanics, 40*(1), 54–59.
4. Harding, J., Wood, E. O., & Campbell, J. D. (1960). Tensile testing of materials at impact rates of strain. *Journal Mechanical Engineering Science, 2*(2), 88–96.
5. Hauser, F. (1966). Techniques for measuring stress-strain relations at high strain rates. *Experimental Mechanics, 6*(8), 395–402.
6. Ogawa, K. (1984). Impact-tension compression test by using a split-Hopkinson bar. *Experimental Mechanics, 24*(2), 81–86.
7. Lei, N., & Xu, D. (2017). Deformation temperature and material constitutive model of cupronickel B10. *Journal of Mechanical Science and Technology, 31*(8), 3761–3767.
8. Johnson, G. R., Cook, W. H. (1983). A constitutive model and data for metals subjected to large strains, high strain rates, and high temperatures. In *Proceedings of the 7th international symposium on ballistics*, The Hague, Netherlands, 19–21 April, pp. 541–547.
9. Shin, H., & Kim, J.-B. (2016). Understanding the anomalously long duration time of the transmitted pulse from a soft specimen in a kolsky bar experiment. *International Journal of Precision Engineering and Manufacturing, 17*(2), 203–208.
10. Chunzheng, D., Fangyuan, Z., Siwei, Q., Wei, S., & Minjie, W. (2018). Modeling of dynamic recrystallization in white layer in dry hard cutting by finite element-cellular automaton method. *Journal of Mechanical Science and Technology, 32*(9), 4299–4312.
11. Kim, J. T., Sakong, J., Woo, S.-C., Kim, J.-Y., & Kim, T.-W. (2018). Determination of the damage mechanisms in armor structural materials via self-organizing map analysis. *Journal of Mechanical Science and Technology, 32*(1), 129–138.
12. Lindholm, U. S., & Yeakley, L. M. (1968). High strain-rate testing: Tension and compression. *Experimental Mechanics, 8*(1), 1–9.
13. Staab, G. H., & Gillet, A. (1991). A direct-tension split Hopkinson bar for high strain-rate testing. *Experimental Mechanics, 31*(3), 232–235.
14. Bang, H., & Cho, C. (2017). Failure behavior/characteristics of fabric reinforced polymer matrix composite and aluminum6061 on dynamic tensile loading. *Journal of Mechanical Science and Technology, 31*(8), 3661–3664.
15. Huh, H., Kang, W. J., & Han, S. S. (2002). A tension split Hopkinson bar for investigating the dynamic behavior of sheet metal. *Experimental Mechanics, 42*(1), 8–17.
16. Nicholas, T. (1981). Tensile testing of materials at high rates of strain. *Experimental Mechanics, 21*(5), 177–185.
17. Pham, T. N., Choi, H. S., & Kim, J.-B. (2013). A numerical investigation into the tensile split Hopkinson pressure bars test for sheet metals. *Applied Mechanics and Materials, 421*, 464–467.
18. Nguyen, K. H., Kim, H. C., Shin, H., Yoo, Y.-H., & Kim, J.-B. (2017). Numerical investigation into the stress wave transmitting characteristics of threads in the split Hopkinson tensile bar test. *International Journal of Impact Engineering, 109*, 253–263.
19. Prabowo, D. A., Kariem, M. A., & Gunawan, L. (2017). The effect of specimen dimension on the results of the Split-Hopkinson tension bar testing. *Procedia Engineering, 173*, 608–614.
20. Nguyen, K. H. (2018). Numerical investigation into the stress wave transmitting characteristics of threads and specimen design

in the split Hopkinson tensile bar test, Ph. D. thesis, Seoul National University of Science and Technology.

21. Owolabi, G., Odoh, D., Odeshi, A., & Whitworth, H. (2013). Occurrence of dynamic shear bands in AISI 4340 steel under impact loads. *World Journal of Mechanics, 3*, 139–145.

22. Yoo, Y.-H., Paik, S. H., Kim, J.-B., & Shin, H. (2013). Performance of a flying cross bar to incapacitate a long-rod penetrator based on a finite element model. *Engineering with Computers, 29*(4), 409–415.

23. Kim, J.-B., & Shin, H. (2009). Comparison of plasticity models for tantalum and a modification of the PTW model for wide ranges of strain, strain rate, and temperature. *International Journal of Impact Engineering, 36*(5), 746–753.

24. Cha, S.-H., Shin, H., & Kim, J.-B. (2010). Numerical Investigation of Frictional Effects and Compensation of Frictional Effects in Split Hopkinson Pressure Bar (SHPB) Test. *Transactions of the Korean Society of Mechanical Engineers, A, 34*(5), 511–518.

25. Maudlin, P. J., Bingert, J. F., House, J. W., & Chen, S. R. (1999). On the modeling of the Taylor cylinder impact test for orthotropic textured materials: experiments and simulations. *International Journal Plasticity, 15*(2), 139–166.

26. Nemat-Nasser, S., & Isaacs, J. (1997). Direct measurement of isothermal flow stress of metals at elevated temperatures and high strain rates with application to Ta and Ta–W alloys. *Acta Materialia, 45*(3), 907–919.

Khac-Ha Nguyen is an engineer in ARITEC CO., LTD. Korea. His research interest is computational mechanics, computational fluid mechanics, and precision manufacturing."

Chang-Whan Lee received B.S. and Ph. D. in mechanical engineering from KAIST in 2007 and 2014, respectively. He has been an assistant professor in Seoul National University of Science and Technology since 2016. His research interests include simulation and development of the metal forming process, lightweight materials such as magnesium alloy sheets.

Hyunho Shin received BE and ME degrees in Materials Engineering from Korea University, Seoul, Korea, in 1986 and 1988, respectively. In 1994, he received his PhD degree in Materials Engineering from Georgia Institute of Technology, Atlanta, Georgia. He was with Agency for Defense Development, Daejeon, Korea, as a senior researcher from 1996 to 2003. Since 2005, he has been with Gangneung-Wonju National University, Gangneung, Korea, as a tenure-track professor, and he is now a professor of the Department of Materials Engineering. He has authored/co-authored more than 100 of Science-Citation-Indexed journal articles. His areas of interest include material properties for simulation (constitutive, fracture, and EOS models and their calibration) and smart processing for property improvement.
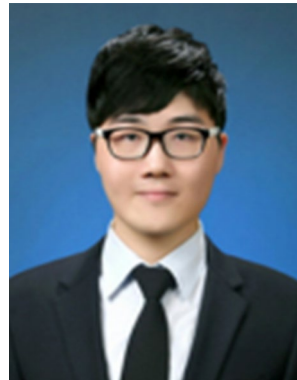
Joo Hyoung Lee is an Engineer in Agency for Defense Development. His research interest is penetration dynamics and numerical simulation

Jong-Bong Kim received the B.S. and M.S. in Precision Engineering from KAIST (Korea Advanced Institute of Science and Technology), Daejon, Korea, in 1993 and 1995, respectively. In 2000, he received his Ph.D. in Mechanical Engineering from Taejon, Korea. Since September 2006, he has been with the Department of Automotive Engineering, SeoulTech (Seoul National University of Science and Technology), Seoul, Korea, where became an Associate Professor in 2012. His areas of interest include high-strain rate deformation behaviors of solids and structures, high-strain-rate constitutive equations, penetration analysis of projectiles, active protection systems, and dynamic collision analysis.